

Electronic Supplementary Information (ESI)

Dinuclear Zirconium Complex Bearing 1,5-Bridged-Calix[8]arene Ligand as Effective Catalyst for the Synthesis of Macrolactones

Rosita Lapenta,^a Nicola Alessandro De Simone,^a Antonio Buonerba,^{a,b,} Carmen Talotta,^{a*} Carmine Gaeta,^a Placido Neri,^a Alfonso Grassi^{a,b} and Stefano Milione^{a,b}*

^a Dipartimento di Chimica e Biologia, Università degli Studi di Salerno, via Giovanni Paolo II, 84084 Fisciano (SA), Italy

^b Interuniversity Consortium Chemical Reactivity and Catalysis, CIRCC, via Celso Ulpiani 27, 70126 (BA), Italy.

* Correspondence should be addressed to: A.B.: abuonerba@unisa.it; C.T.: ctalotta@unisa.it

Table of Contents

1. NMR Characterization	S4
Figure S1. ^1H NMR spectrum of C (600 MHz, pyridine- d_5 , 25 °C).	S4
Figure S2. ^1H - ^1H COSY spectrum (600 MHz, pyridine- d_5 , 90°C) of C (a) with magnifications of the diagnostic regions (b-d).	S5
Figure S3. ^1H - ^{13}C HSQC spectrum (600 MHz, pyridine- d_5 , 25°C) of the complex C (a) with magnifications of the diagnostic regions (b-d).	S6
Figure S4. ^1H - ^1H NOESY spectrum (600 MHz, pyridine- d_5 , 90°C) of the complex C (a) with magnifications of the diagnostic regions (b-d).	S7
Figure S5. DEPT135 (a) and ^{13}C NMR (b) spectra (600 MHz, pyridine- d_5 , 90°C) of the complex C (Scheme 1).	S8
Figure S6. DOSY NMR spectra of the complex C (600 MHz, 25°C, benzene- d_6) (a) and of C (600 MHz, 25°C, benzene- d_6) in presence of the internal standard S as reference (b). Diffusion coefficients: $\text{C} = 5.6 \cdot 10^{-8} \pm 4.6 \cdot 10^{-10} \text{ m}^2\text{s}^{-1}$; $\text{S} = 6.4 \cdot 10^{-8} \pm 3.9 \cdot 10^{-10} \text{ m}^2\text{s}^{-1}$	S9
Figure S7. Possible configurations of the ligand L with C_{2v} symmetry (a-d) and the structure of the complex C , compatible with NMR information, resulting from the configuration in b.	S10
Figure S8. ^1H - ^1H COSY spectrum (600 MHz, benzene- d_6 , 25°C) of C' (a) with magnifications of the diagnostic regions (b-d).	S11
Figure S9. ^1H - ^{13}C HSQC spectrum (600 MHz, benzene- d_6 , 25°C) of the complex C' (a) with magnifications of the diagnostic regions (b-d).	S12
Figure S10. ^{13}C NMR spectrum of the complex C' with diagnostic signal labelled (600 MHz, benzene- d_6 , 25°C).	S13
Figure S11. DOSY NMR spectra of the complex C' (a) and of C' in presence of the internal standard S' as reference (b). Diffusion coefficients: $\text{C} = 4.30 \cdot 10^{-10} \pm 8.56 \cdot 10^{-13} \text{ m}^2\text{s}^{-1}$; $\text{S} = 4.35 \cdot 10^{-10} \pm 5.68 \cdot 10^{-13} \text{ m}^2\text{s}^{-1}$	S14
Figure S12. ^1H NMR spectrum of cyclic PLA synthesized by C (entry 4 of Table 1; CDCl_3 , 300 MHz, 25°C).	S15
Figure S13. ^1H NMR spectrum of linear PLA synthesized by C' (entry 9 of Table 1; CDCl_3 , 300 MHz, 25°C).	S15
2. UV-Vis Analysis.....	S16
Figure S14. UV-Vis spectrum of C ($5.8 \cdot 10^{-3}$ M; pyridine; 25 °C; $\epsilon_{436} = 166 \text{ Lmol}^{-1}\text{cm}^{-1}$).	S16
3. ESI-MS and MALDI-MS Analyses	S17
Figure S15. ESI-MS spectrum of the complex C (toluene/methanol solvents mixture).	S17
Figure S16. ESI-MS spectrum of the complex C' (toluene/methanol solvents mixture).	S17
4. Kinetic Investigations.....	S18

Figure S17. Polymerization of <i>rac</i> -LA catalyzed by C (a) with the corresponding plot of $\ln([LA]_0/[LA])$ versus time.....	S18
Figure S18. Plot of number-averaged molecular weights $M_{n(\text{exp})}$ (square) vs monomer to initiator ratio with theoretical molecular weights $M_{n(\text{th})}$ (dots) for LA polymerization catalyzed by C (reaction conditions in Table 1).....	S19
Figure S19. Polymerization of <i>rac</i> -LA catalyzed by C' (a) with the corresponding plot of $\ln([LA]_0/[LA])$ versus time.....	S20
Table S1. Reaction rate as a function of catalyst concentration for ROP of LA with C	S21
5. Gel Permeation Chromatography.	S22
Figure S20. Gel permeation chromatogram of the polymer sample from entry 1 of Table 1	S22
Figure S21. Gel permeation chromatogram of the polymer sample from entry 2 of Table 1	S22
Figure S22. Gel permeation chromatogram of the polymer sample from entry 3 of Table 1	S23
Figure S23. Gel permeation chromatogram of the polymer sample from entry 4 of Table 1	S23
Figure S24. Gel permeation chromatogram of the polymer sample from entry 5 of Table 1	S24
Figure S25. Gel permeation chromatogram of the polymer sample from entry 6 of Table 1	S24
Figure S26. Gel permeation chromatogram of the polymer sample from entry 7 of Table 1	S25
Figure S27. Gel permeation chromatogram of the polymer sample from entry 8 of Table 1	S25
Figure S28. Gel permeation chromatogram of the polymer sample from entry 9 of Table 1	S26
Figure S29. Gel permeation chromatogram of the polymer sample from entry 10 of Table 1	S26
Figure S30. Gel permeation chromatogram of the polymer sample from entry 11 of Table 1	S27

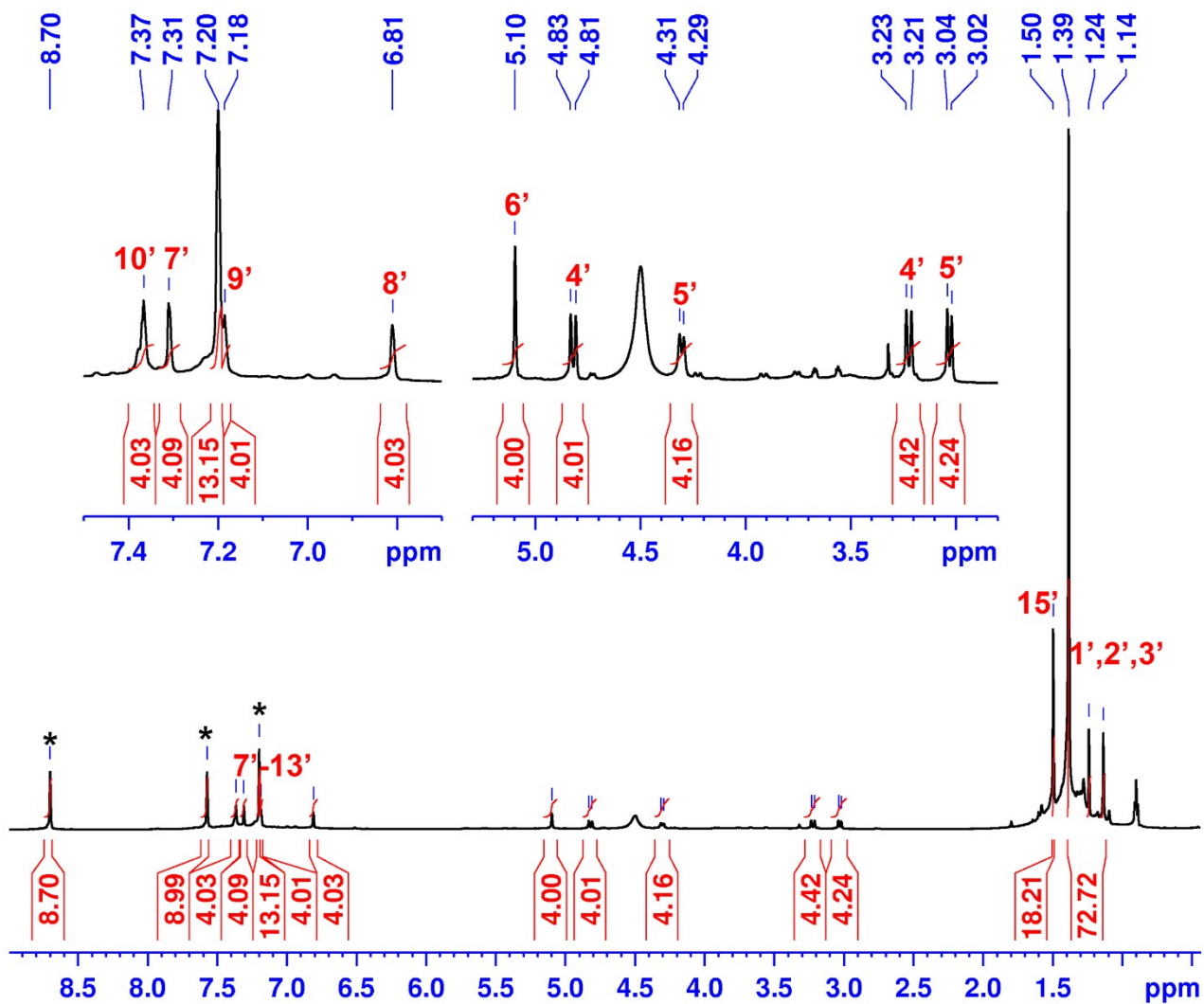
1. NMR CHARACTERIZATION

Figure S1. ¹H NMR spectrum of C (600 MHz, pyridine-*d*₅, 25 °C).

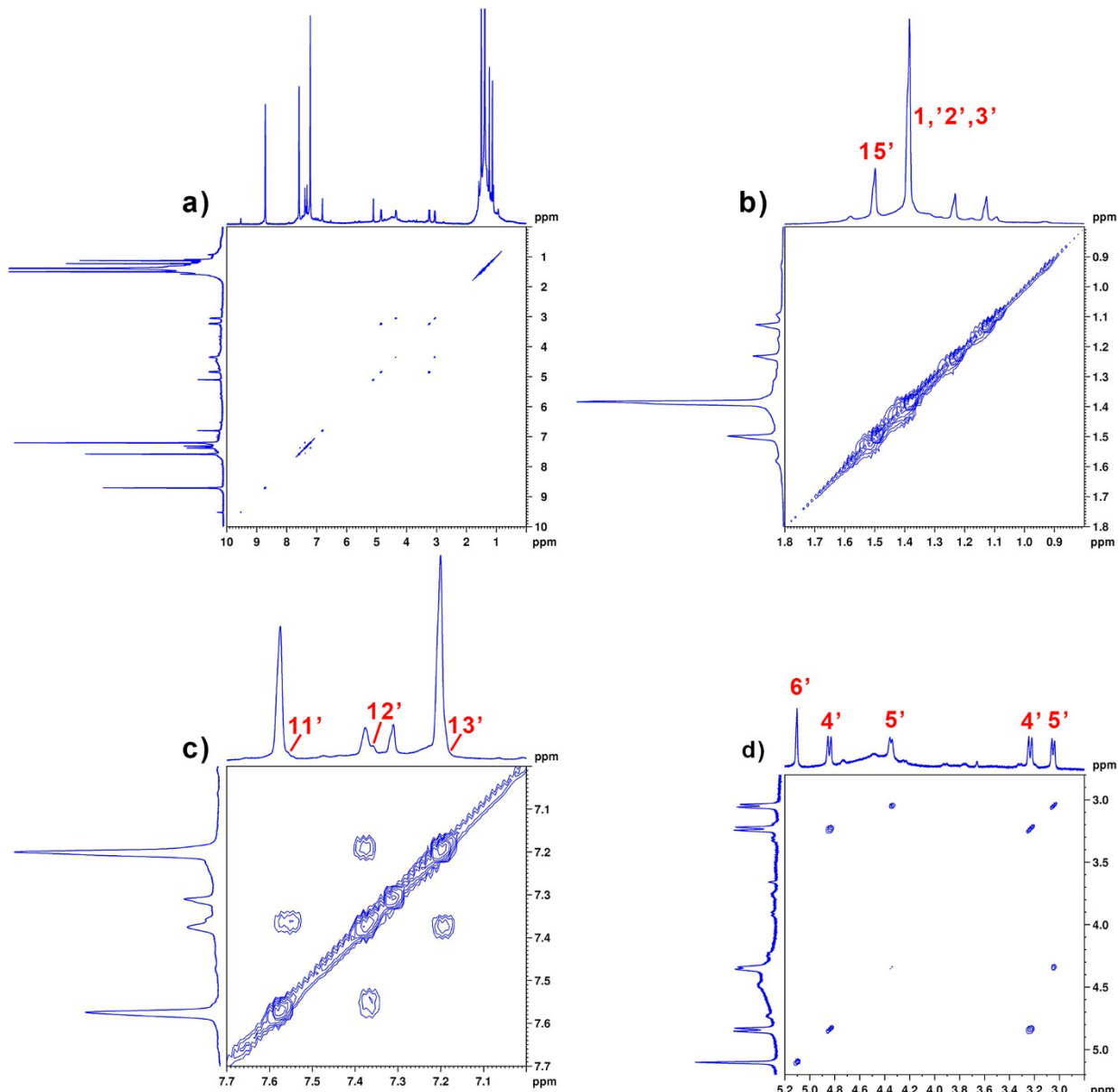


Figure S2. ¹H-¹H COSY spectrum (600 MHz, pyridine-*d*₅, 90°C) of **C** (a) with magnifications of the diagnostic regions (b-d).

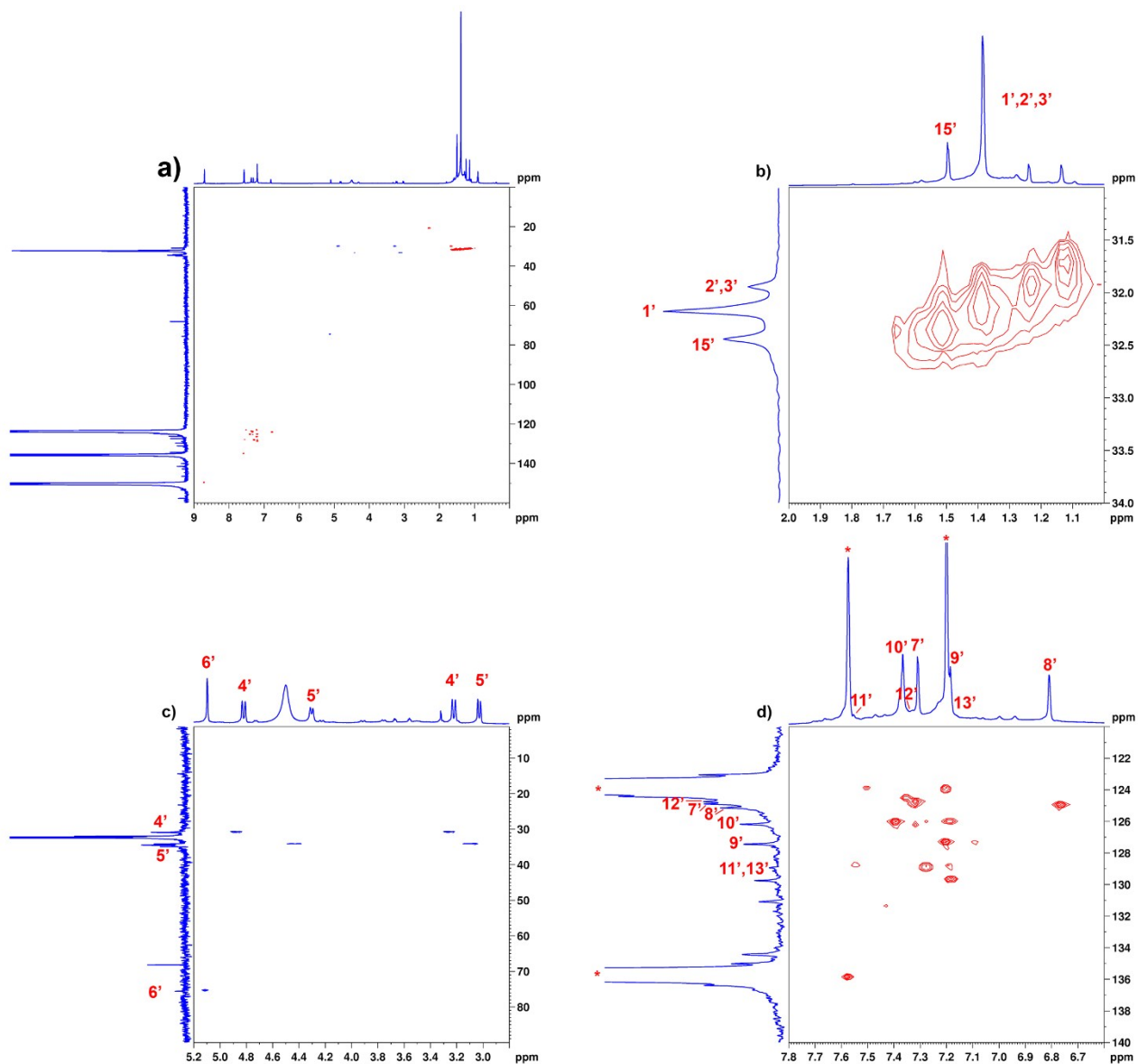


Figure S3. ¹H-¹³C HSQC spectrum (600 MHz, pyridine-*d*₅, 25°C) of the complex C (a) with magnifications of the diagnostic regions (b-d).

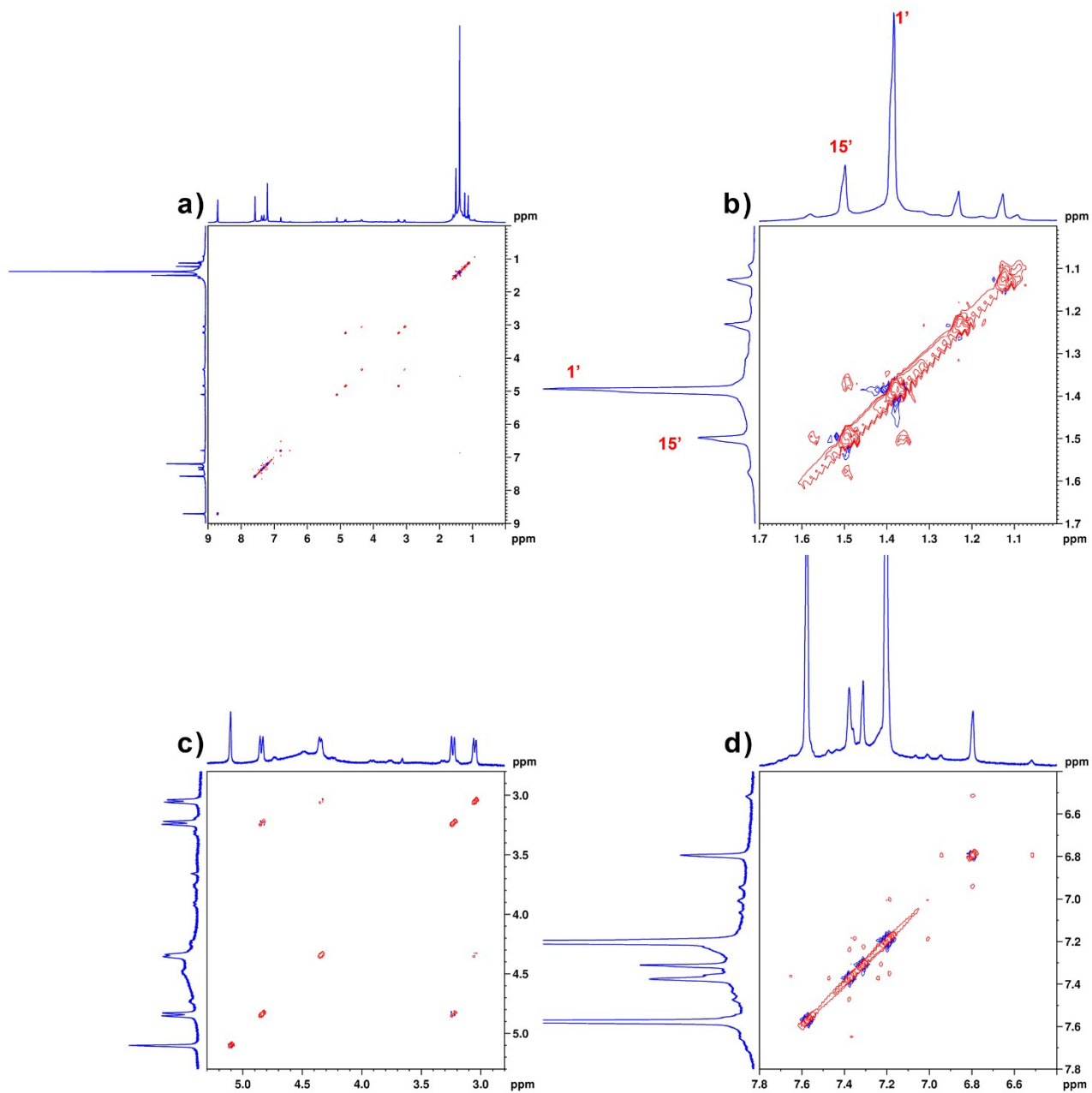


Figure S4. ¹H-¹H NOESY spectrum (600 MHz, pyridine-*d*₅, 90°C) of the complex **C** (a) with magnifications of the diagnostic regions (b-d).

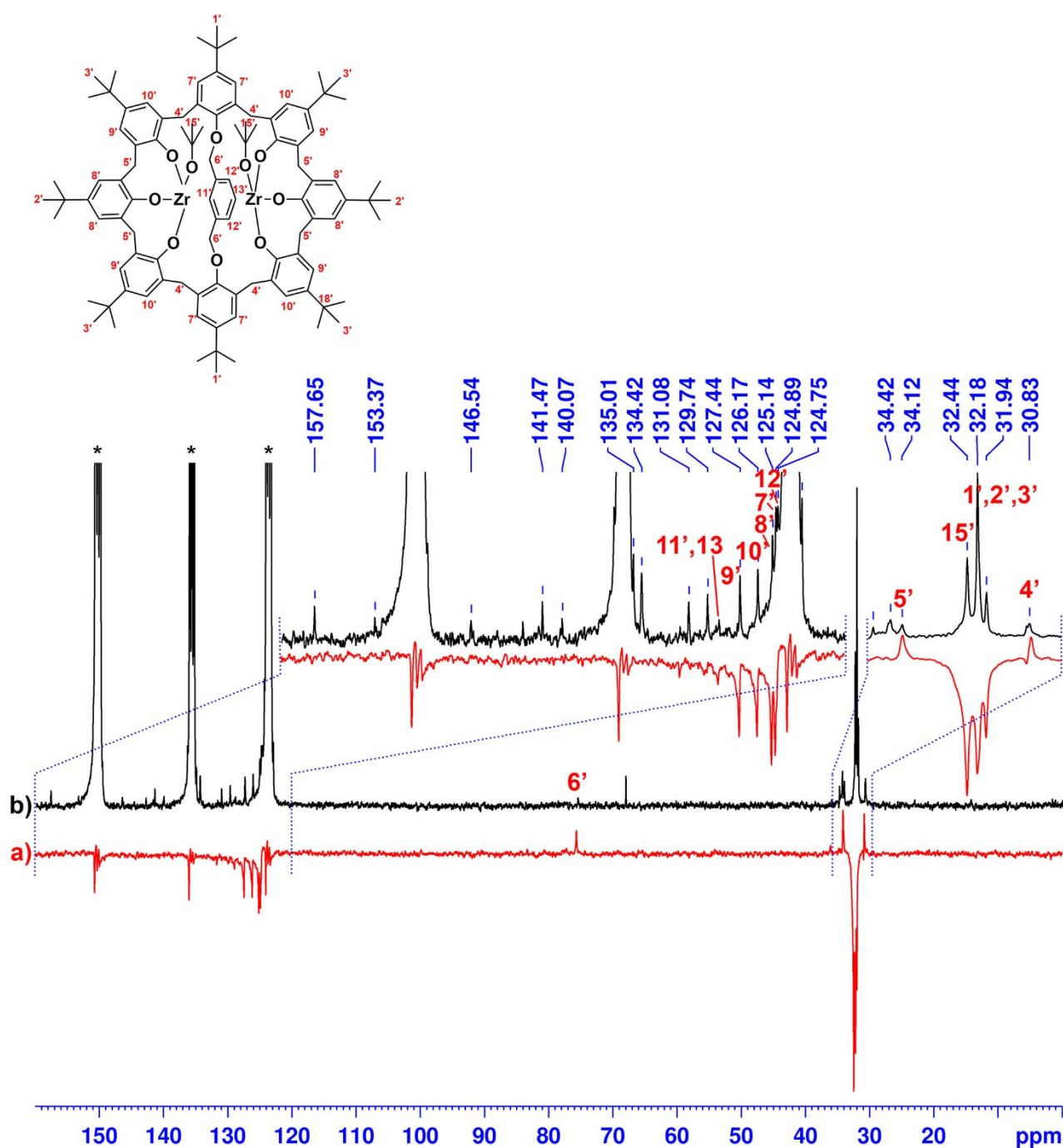


Figure S5. DEPT135 (a) and ¹³C NMR (b) spectra (600 MHz, pyridine-*d*₅, 90°C) of the complex **C** (Scheme 1).

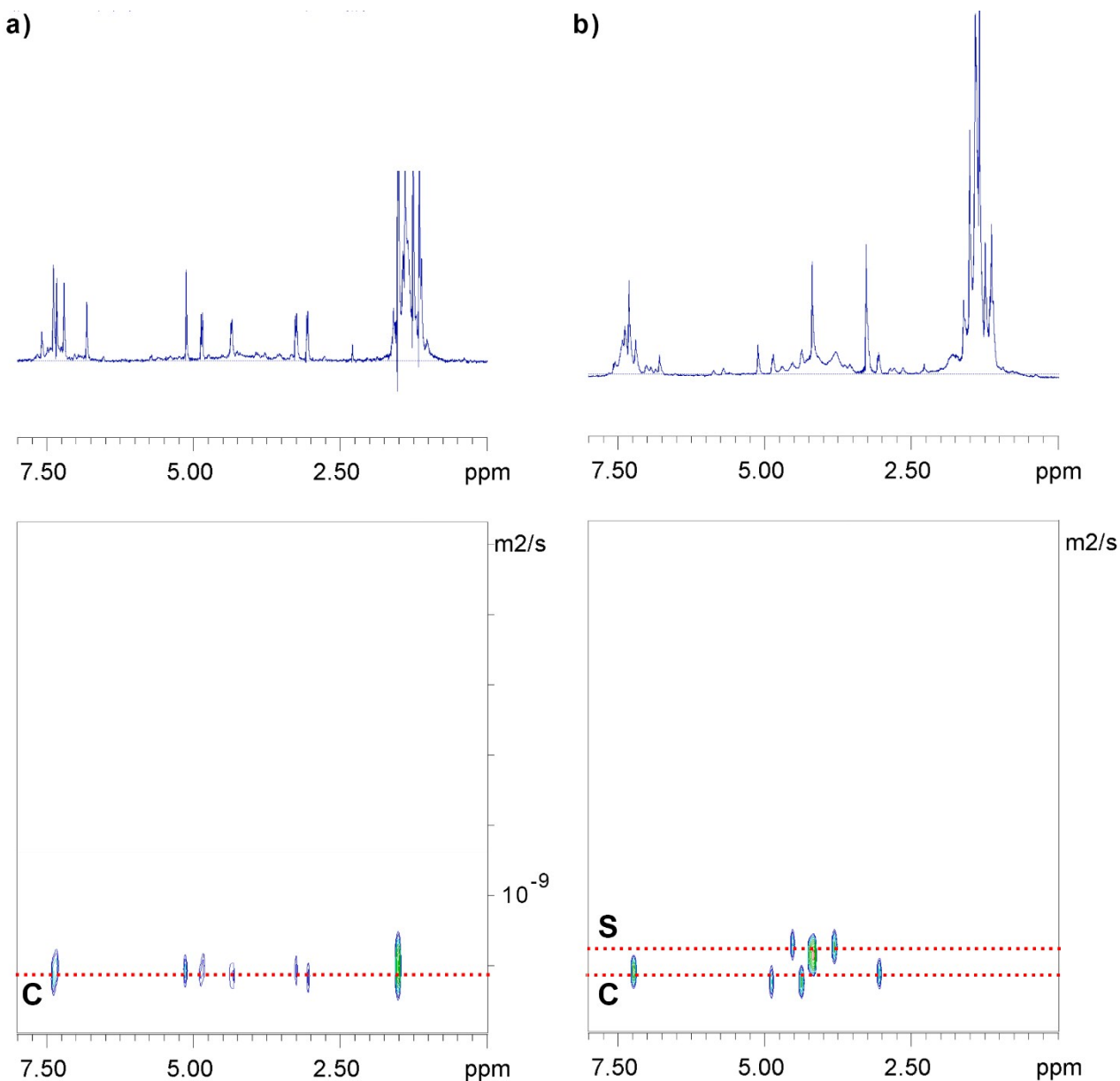


Figure S6. DOSY NMR spectra of the complex **C** (600 MHz, 25°C, benzene-*d*₆) (a) and of **C** (600 MHz, 25°C, benzene-*d*₆) in presence of the internal standard **S** as reference (b). Diffusion coefficients: **C** = $5.6 \cdot 10^{-8} \pm 4.6 \cdot 10^{-10} \text{ m}^2\text{s}^{-1}$; **S** = $6.4 \cdot 10^{-8} \pm 3.9 \cdot 10^{-10} \text{ m}^2\text{s}^{-1}$.

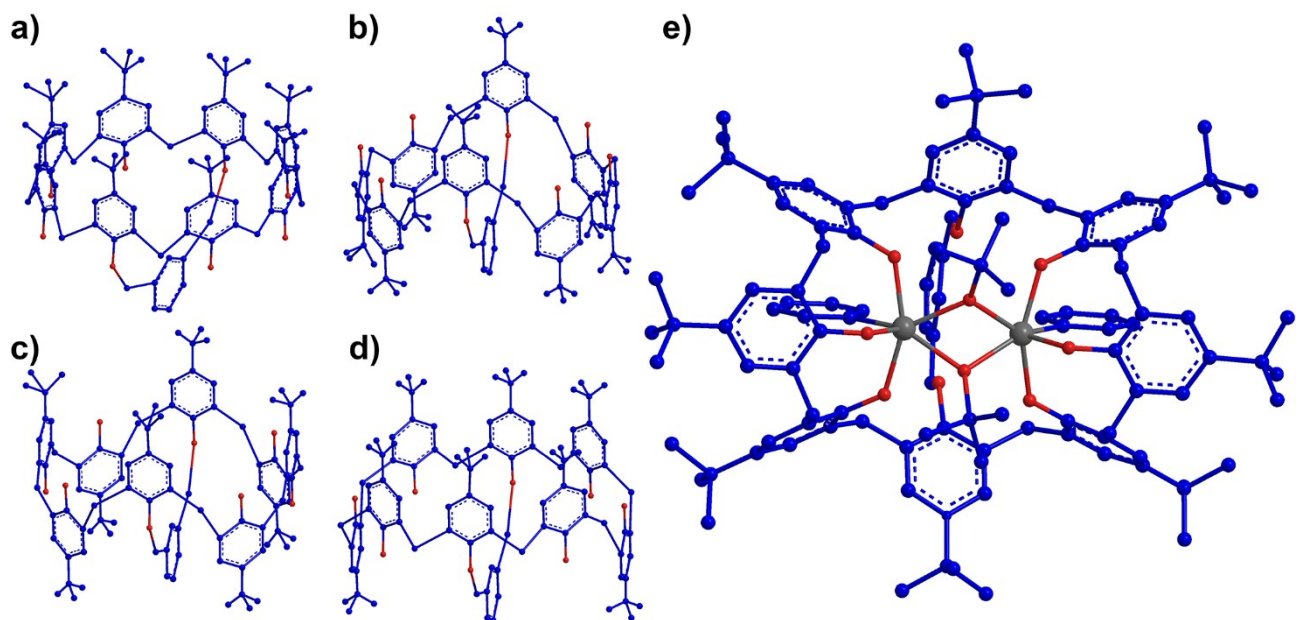


Figure S7. Possible configurations of the ligand **L** with C_{2v} symmetry (a-d) and the structure of the complex **C**, compatible with NMR information, resulting from the configuration in b).

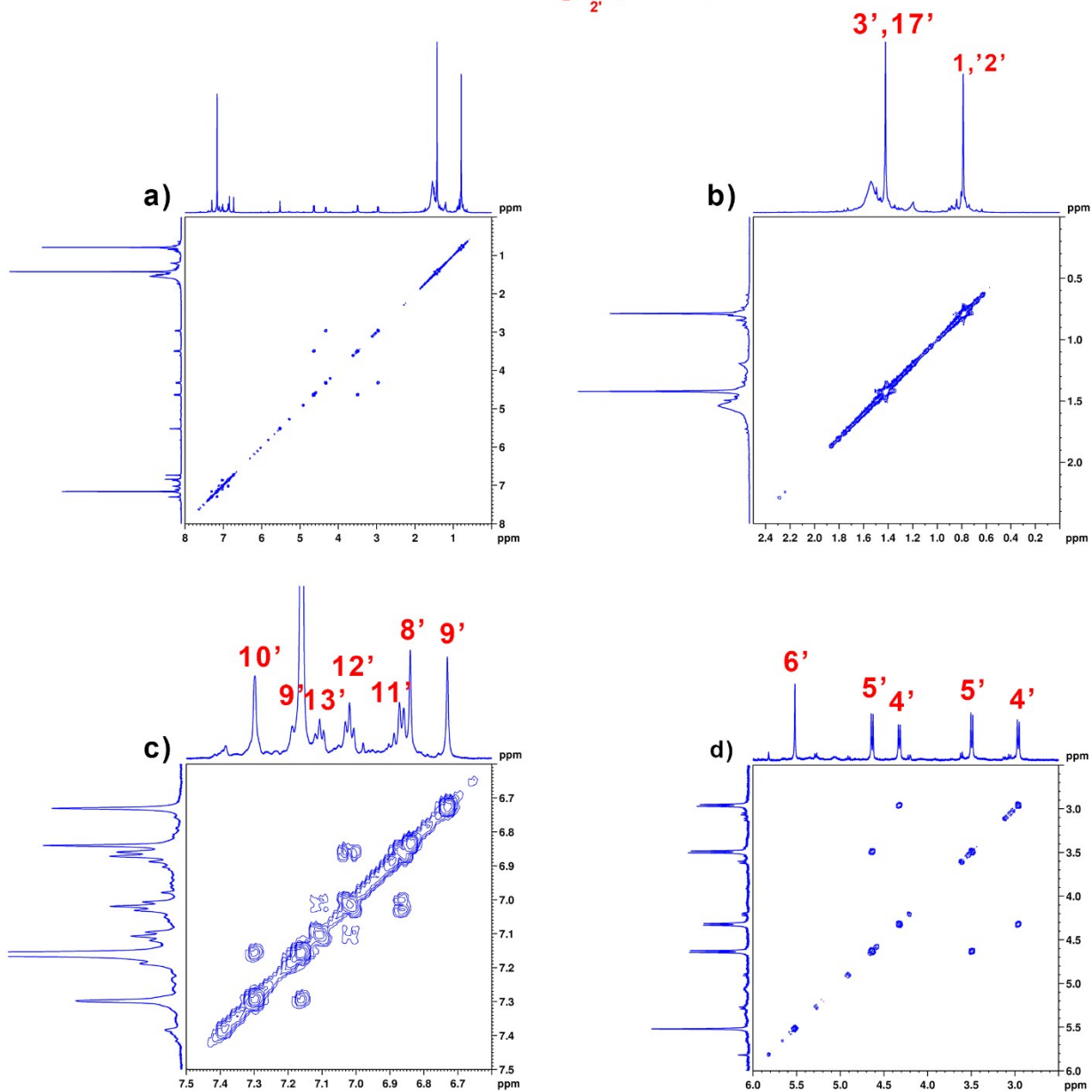
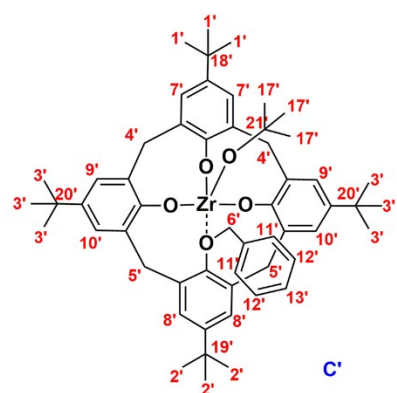


Figure S8. ^1H - ^1H COSY spectrum (600 MHz, benzene- d_6 , 25°C) of **C'** (a) with magnifications of the diagnostic regions (b-d).

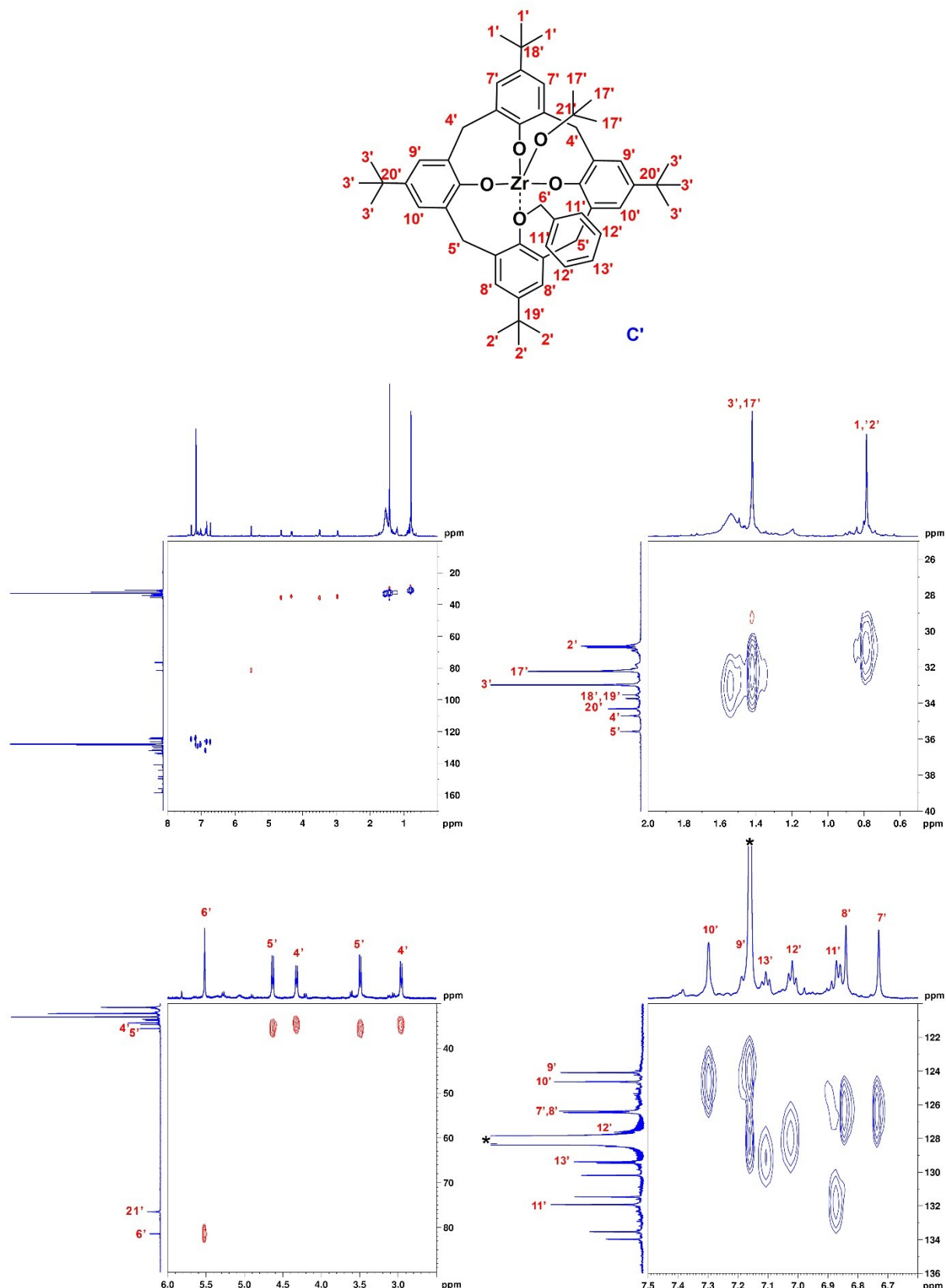


Figure S9. ^1H - ^{13}C HSQC spectrum (600 MHz, benzene- d_6 , 25°C) of the complex **C'** (a) with magnifications of the diagnostic regions (b-d).

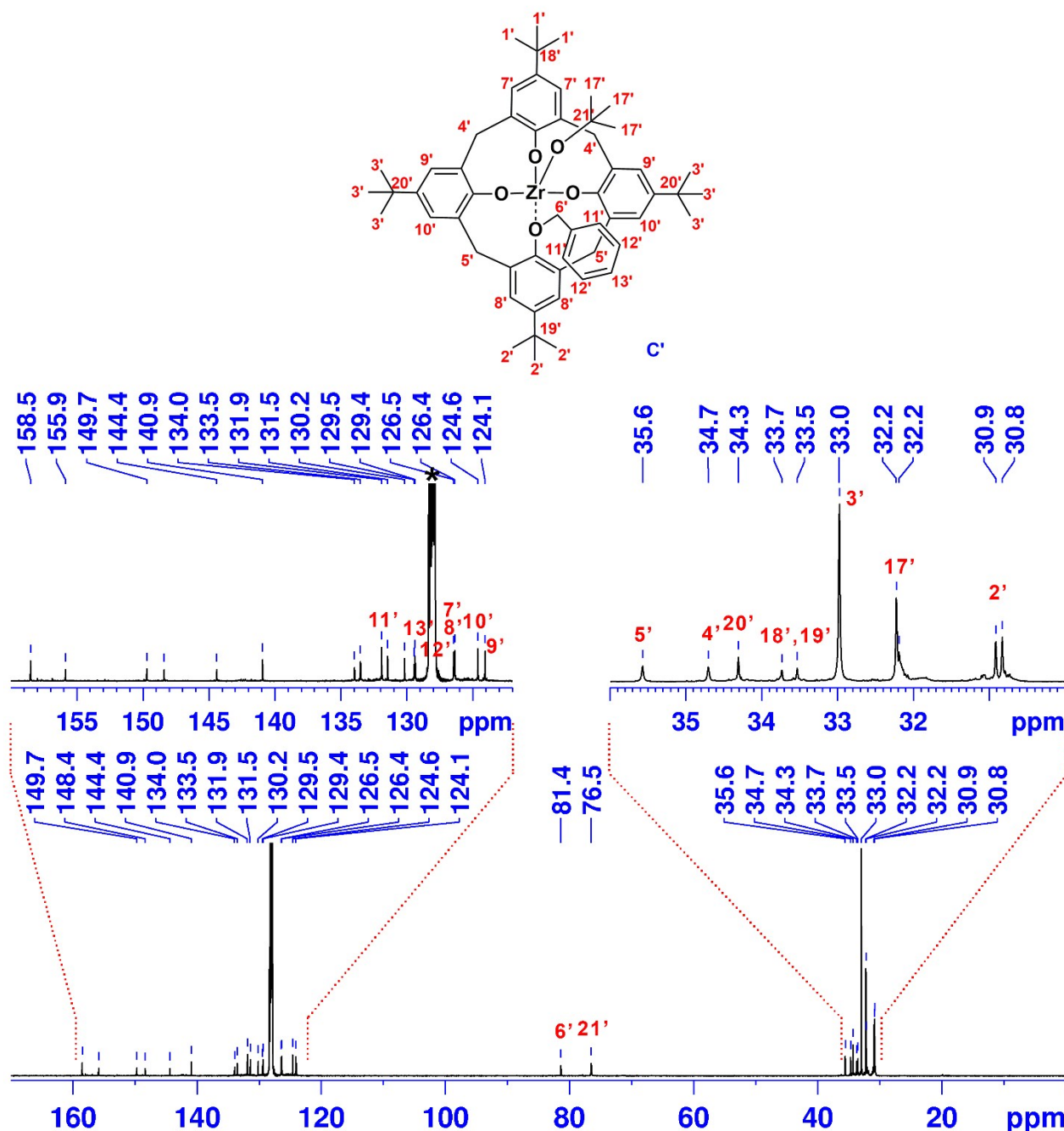


Figure S10. ^{13}C NMR spectrum of the complex \mathbf{C}' with diagnostic signal labelled (600 MHz, benzene- d_6 , 25°C).

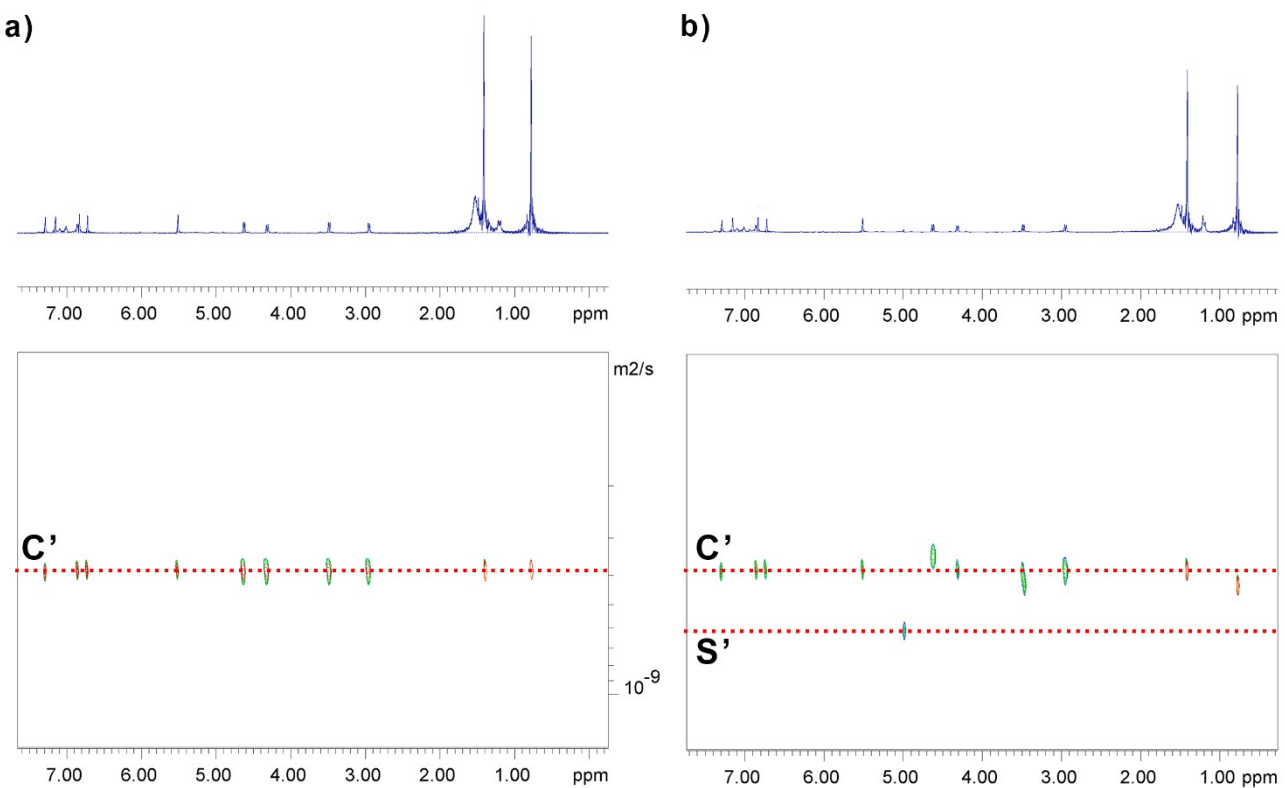


Figure S11. DOSY NMR spectra of the complex **C'** (a) and of **C'** in presence of the internal standard **S'** as reference (b). Diffusion coefficients: $C = 4.30 \cdot 10^{-10} \pm 8.56 \cdot 10^{-13} \text{ m}^2\text{s}^{-1}$; $S = 4.35 \cdot 10^{-10} \pm 5.68 \cdot 10^{-13} \text{ m}^2\text{s}^{-1}$.

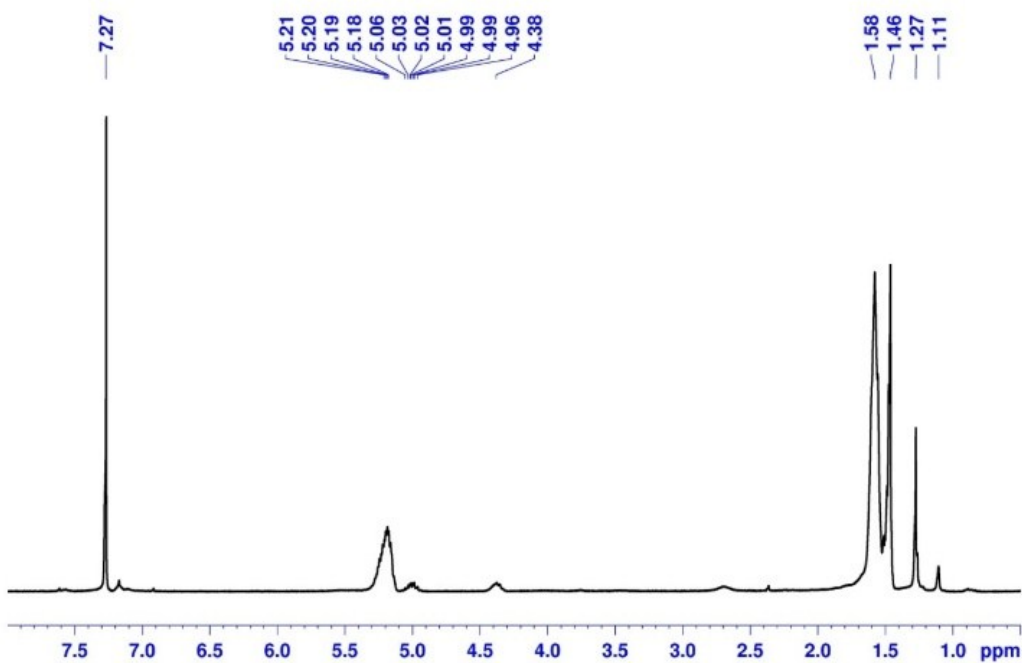


Figure S12. ¹H NMR spectrum of cyclic PLA synthesized by C (entry 4 of Table 1; CDCl₃, 300 MHz, 25°C).

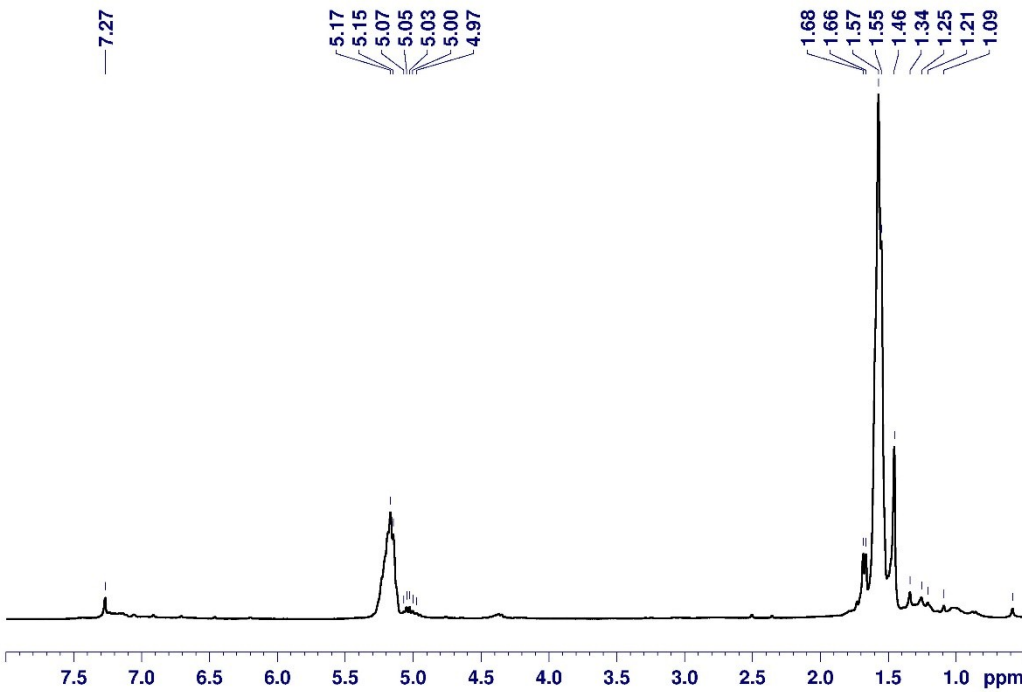


Figure S13. ¹H NMR spectrum of linear PLA synthesized by C' (entry 9 of Table 1; CDCl₃, 300 MHz, 25°C).

2. UV-VIS ANALYSIS

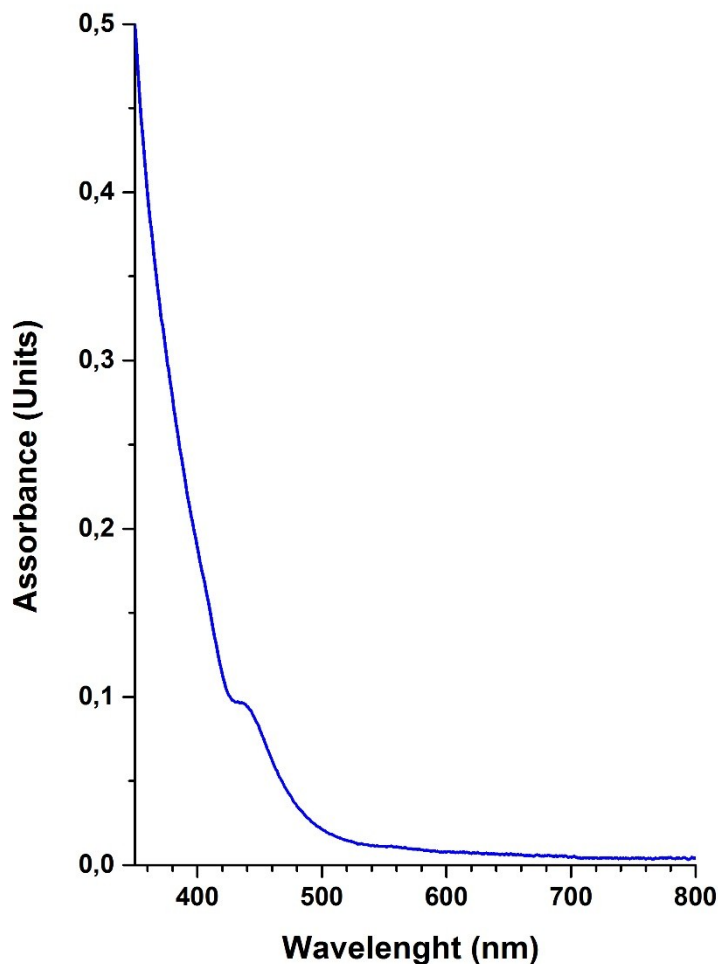


Figure S14. UV-Vis spectrum of **C** ($5.8 \cdot 10^{-3}$ M; pyridine; 25 °C; $\varepsilon_{436} = 166 \text{ Lmol}^{-1}\text{cm}^{-1}$).

3. ESI-MS AND MALDI-MS ANALYSES

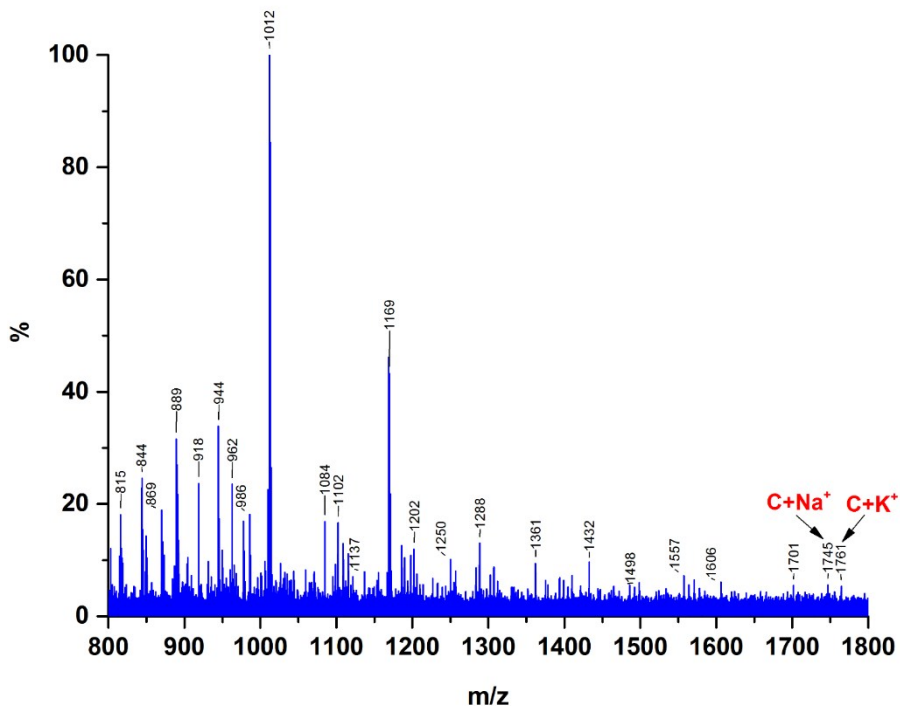


Figure S15. ESI-MS spectrum of the complex **C** (toluene/methanol solvents mixture).

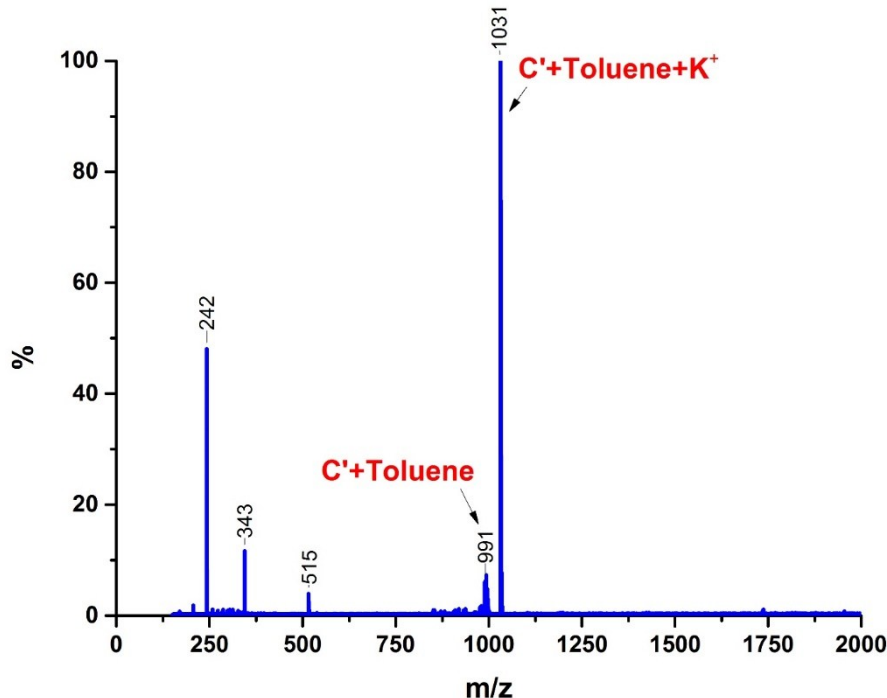


Figure S16. ESI-MS spectrum of the complex **C'** (toluene/methanol solvents mixture).

4. Kinetic Investigations

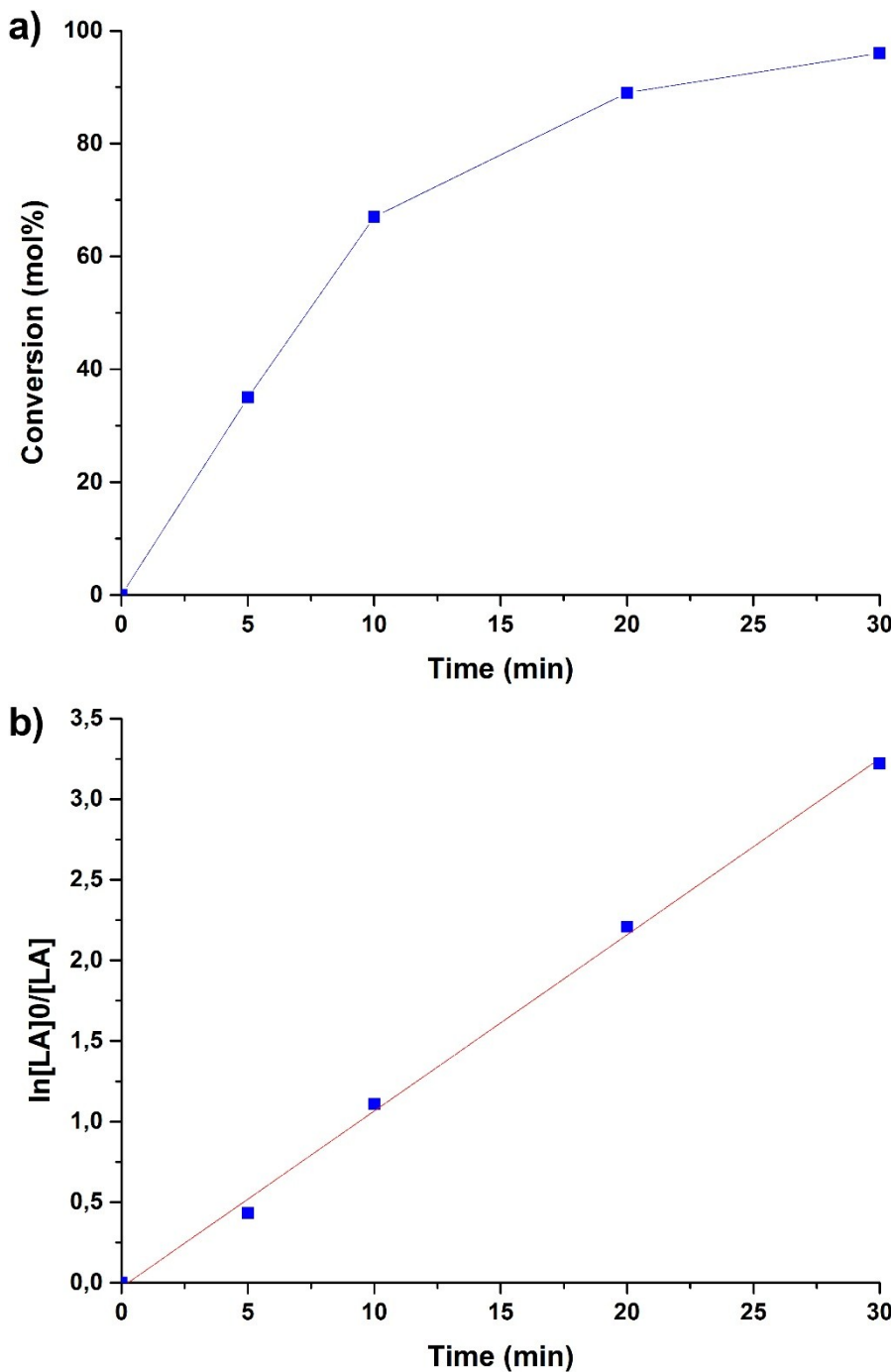


Figure S17. Polymerization of *rac*-LA catalyzed by C (a) with the corresponding plot of $\ln([LA]_0/[LA])$ versus time.

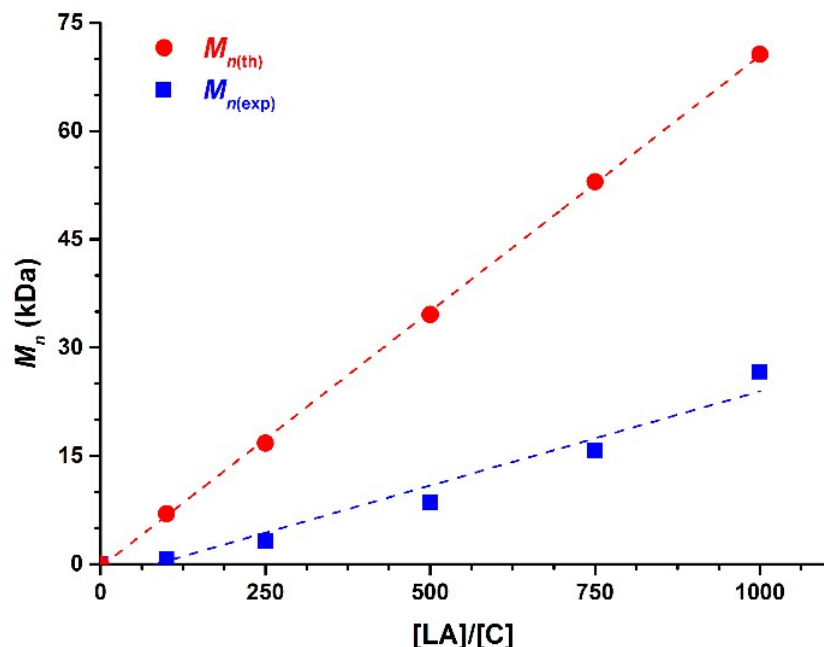


Figure S18. Plot of number-averaged molecular weights $M_{n(\text{exp})}$ (square) vs monomer to initiator ratio with theoretical molecular weights $M_{n(\text{th})}$ (dots) for LA polymerization catalyzed by **C** (reaction conditions in Table 1).

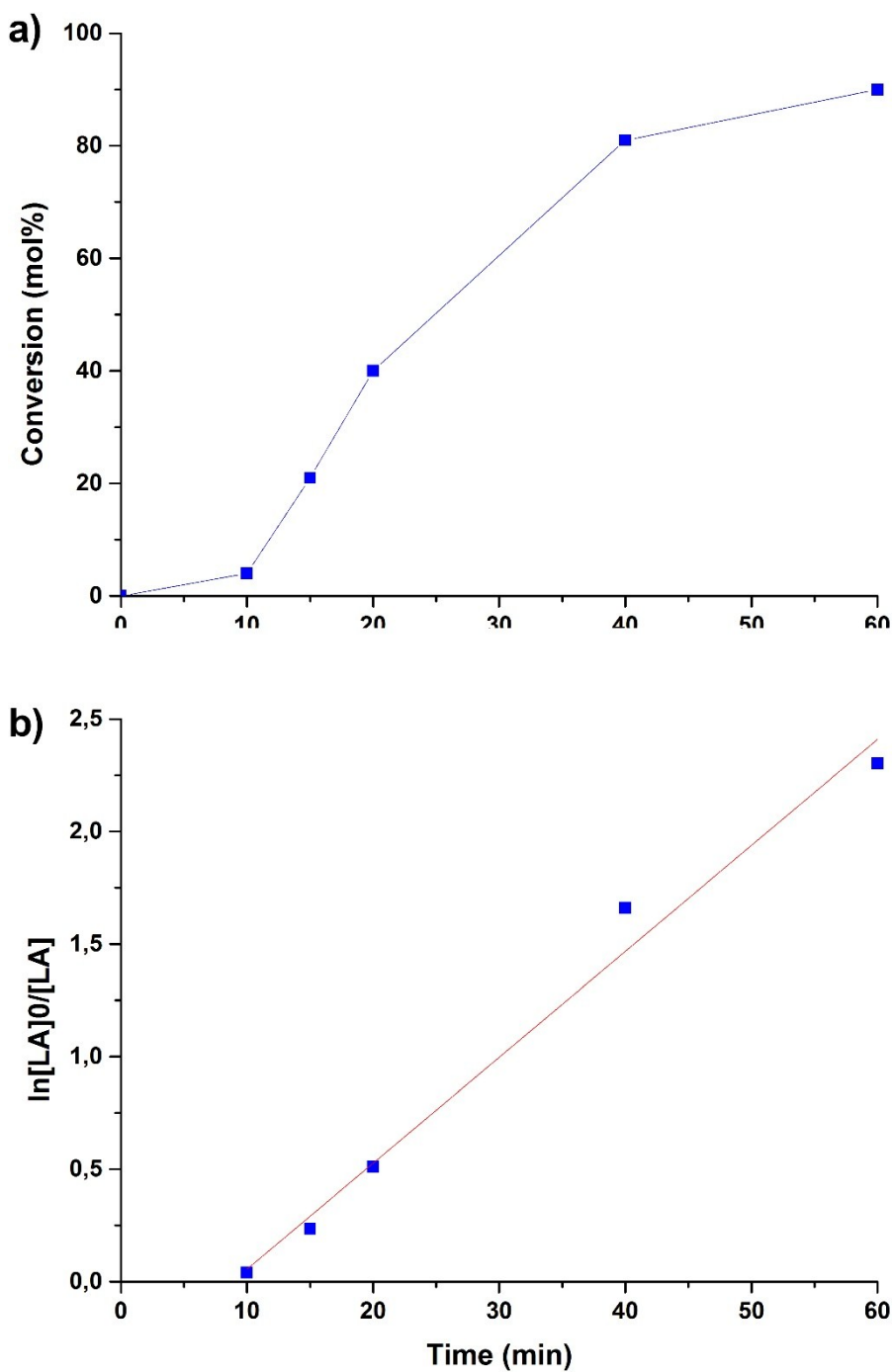


Figure S19. Polymerization of *rac*-LA catalyzed by C' (a) with the corresponding plot of $\ln([LA]_0/[LA])$ versus time.

Table S1. Reaction rate as a function of catalyst concentration for ROP of LA with C.

Entry	[C] (M)	[rac-LA]/[C] (molar ratio)	r (M s⁻¹)
S1	$1.42 \cdot 10^{-2}$	50	$2.7 \cdot 10^{-3} \pm 1.5 \cdot 10^{-4}$
S2	$7.07 \cdot 10^{-3}$	100	$1.7 \cdot 10^{-3} \pm 1.3 \cdot 10^{-4}$
S3	$4.72 \cdot 10^{-3}$	150	$1.2 \cdot 10^{-3} \pm 6.3 \cdot 10^{-5}$
S4	$3.53 \cdot 10^{-3}$	200	$7.3 \cdot 10^{-4} \pm 3.7 \cdot 10^{-5}$

Reaction conditions: [rac-LA] = 0.706 M, TCE-*d*₂ = 0.6 mL, T = 80 °C; reactions carried out inside NMR tubes and monitored with interval of one minute.

5. Gel Permeation Chromatography.

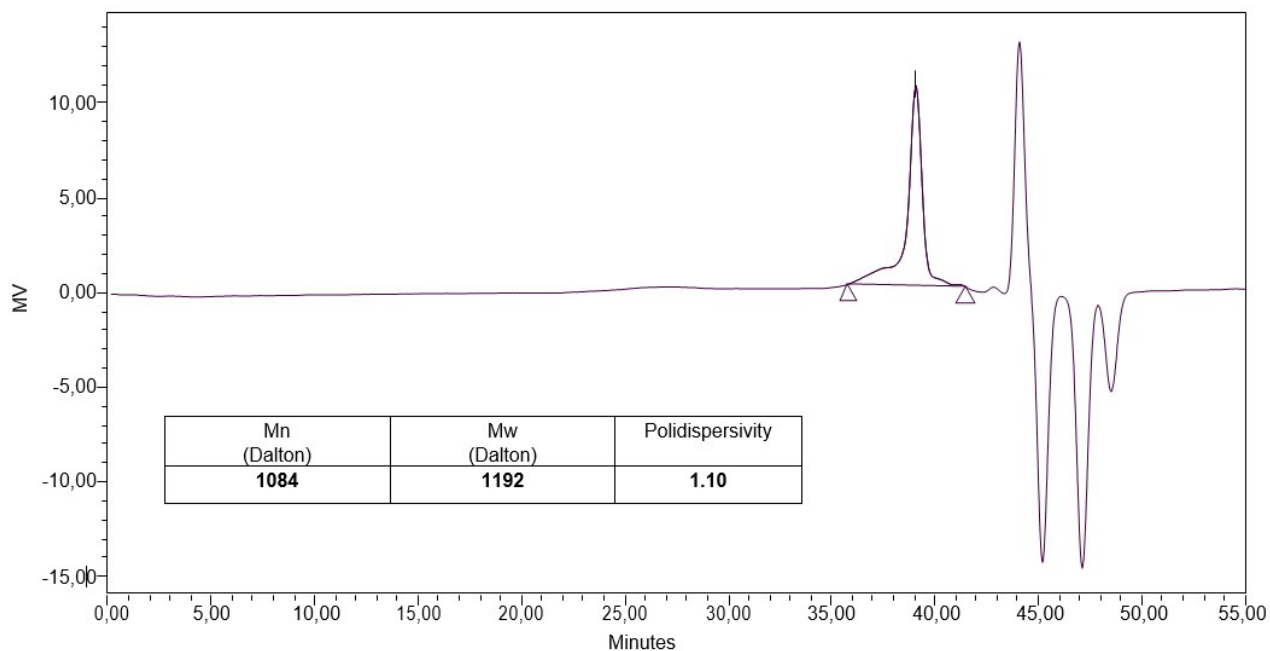


Figure S20. Gel permeation chromatogram of the polymer sample from entry **1** of Table 1.

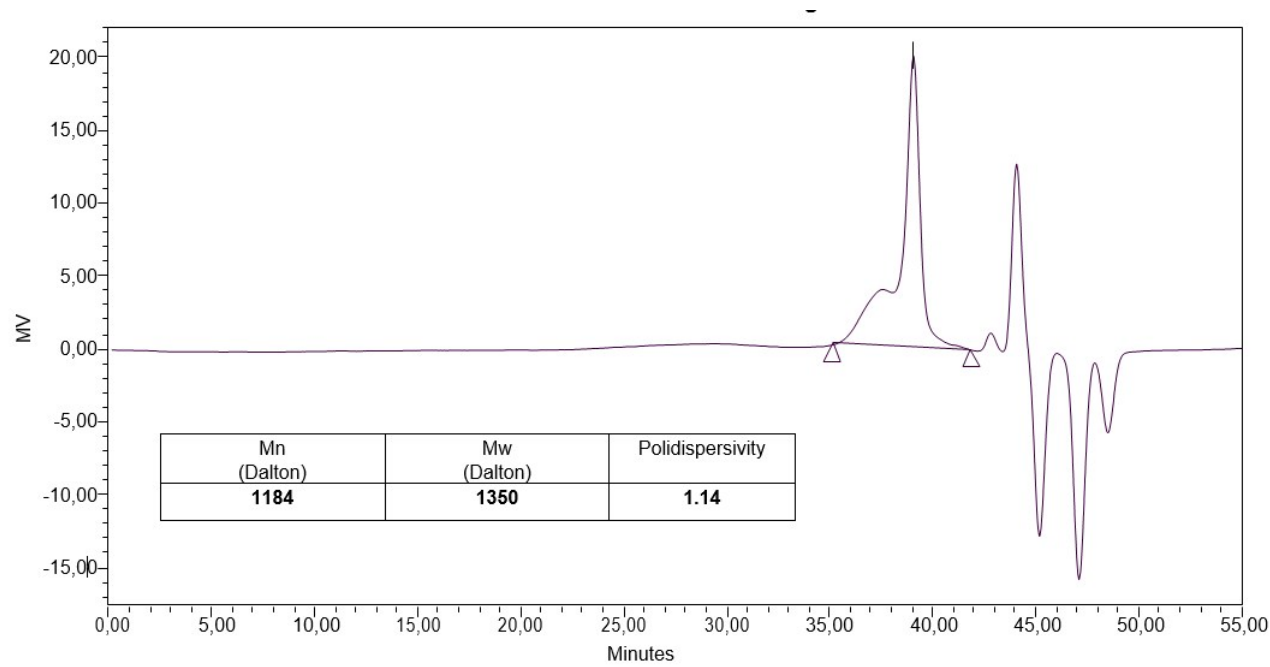


Figure S21. Gel permeation chromatogram of the polymer sample from entry **2** of Table 1.

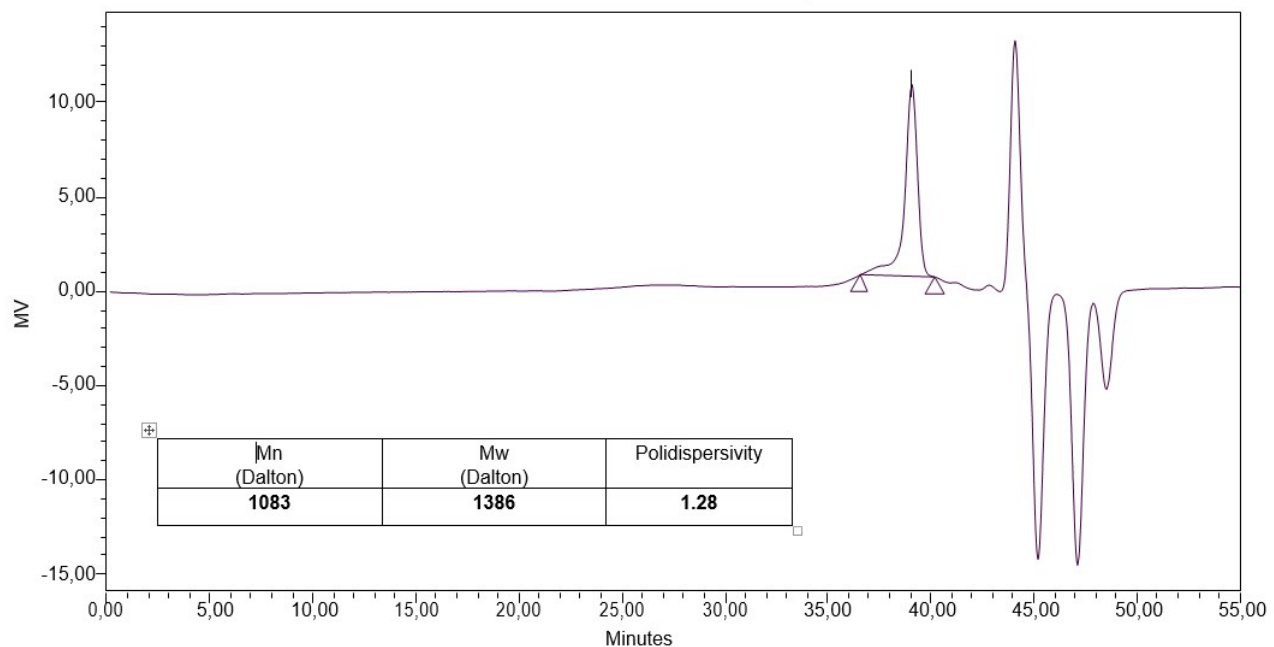


Figure S22. Gel permeation chromatogram of the polymer sample from entry 3 of Table 1.

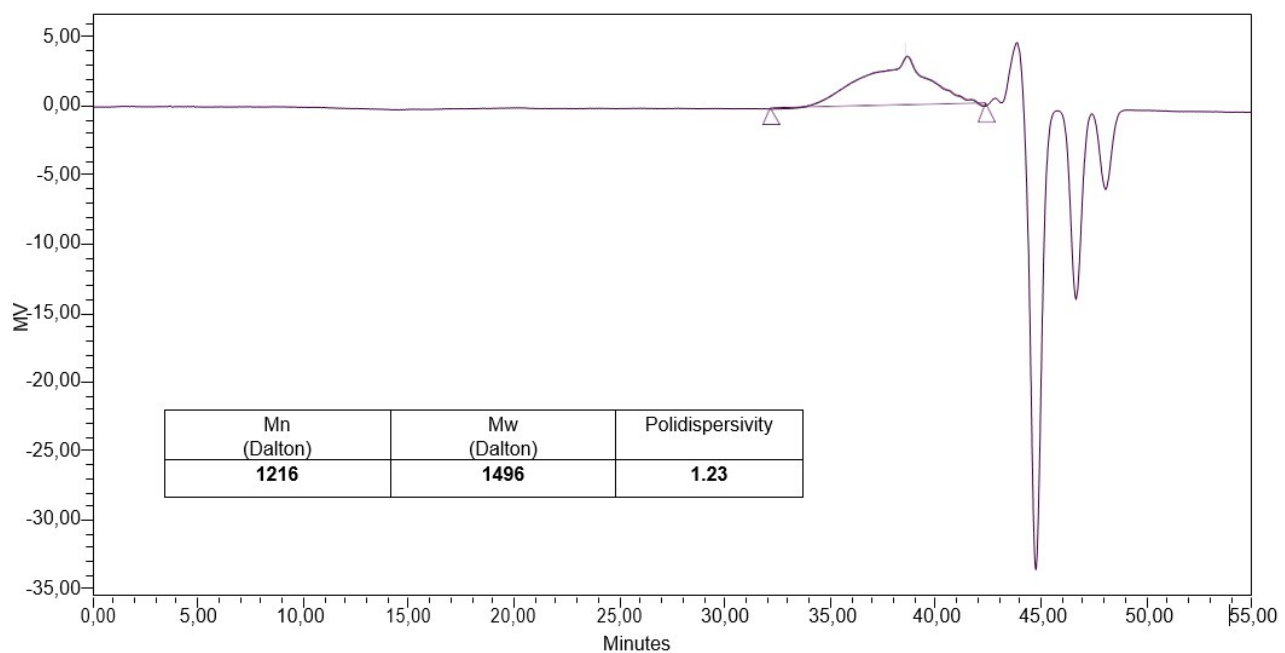


Figure S23. Gel permeation chromatogram of the polymer sample from entry 4 of Table 1.

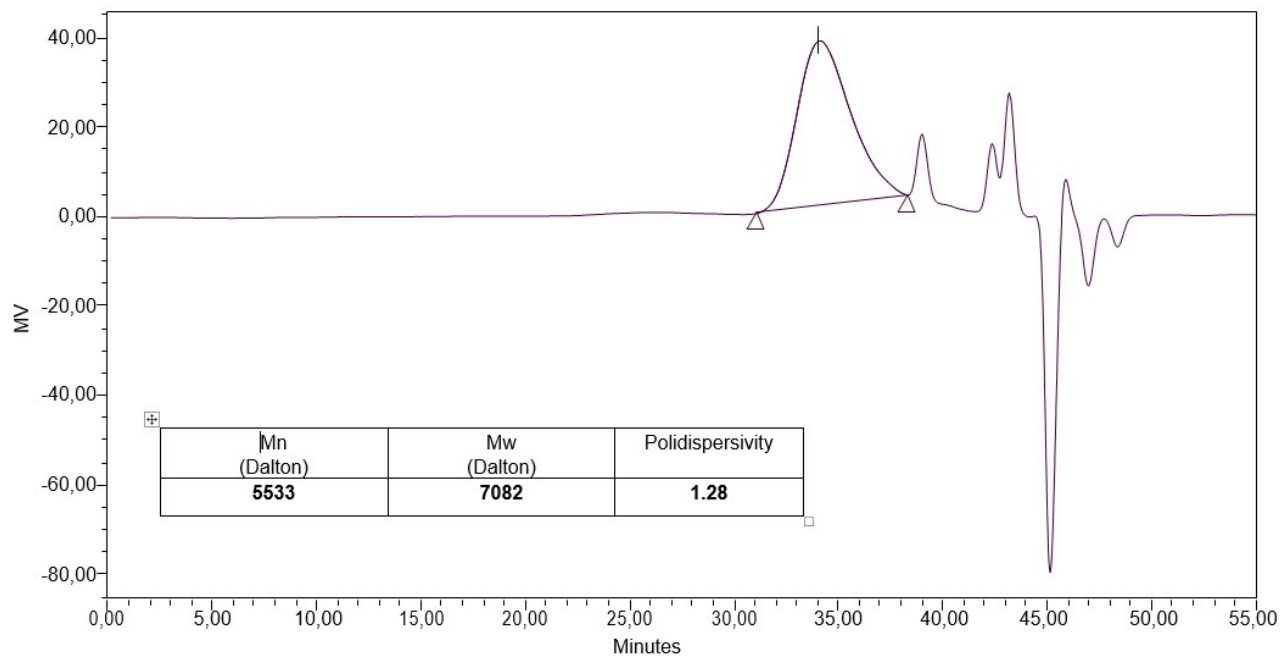


Figure S24. Gel permeation chromatogram of the polymer sample from entry 5 of Table 1.

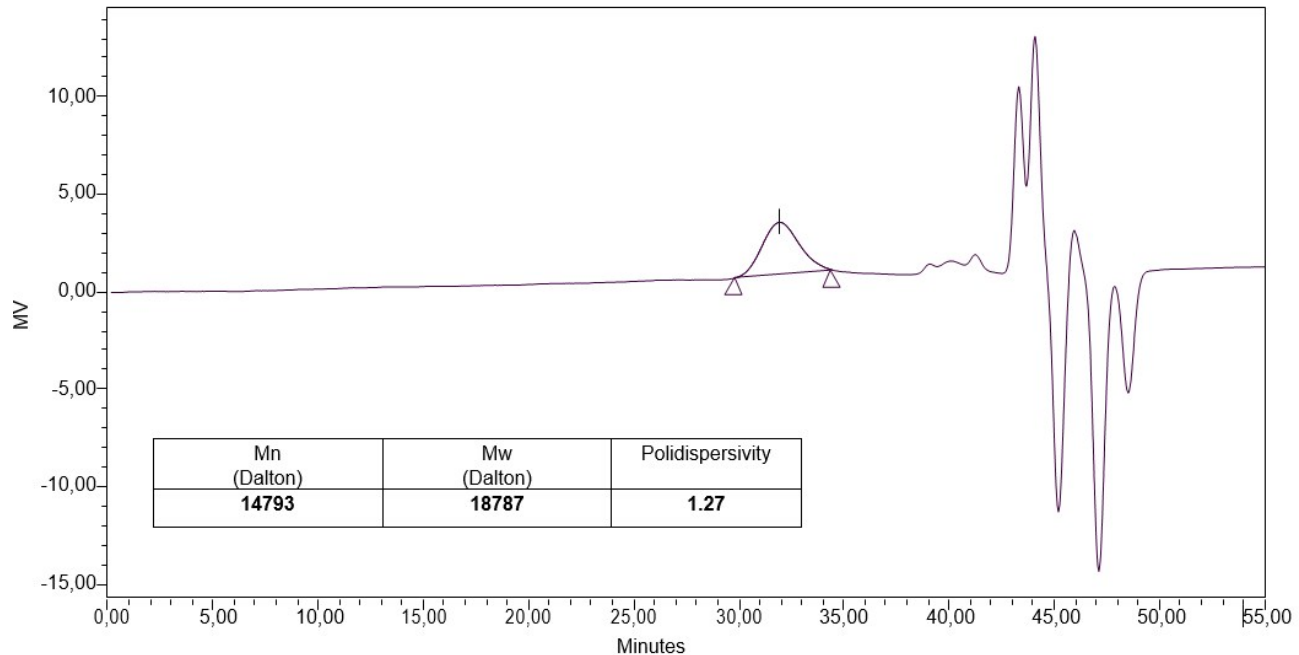


Figure S25. Gel permeation chromatogram of the polymer sample from entry 6 of Table 1.

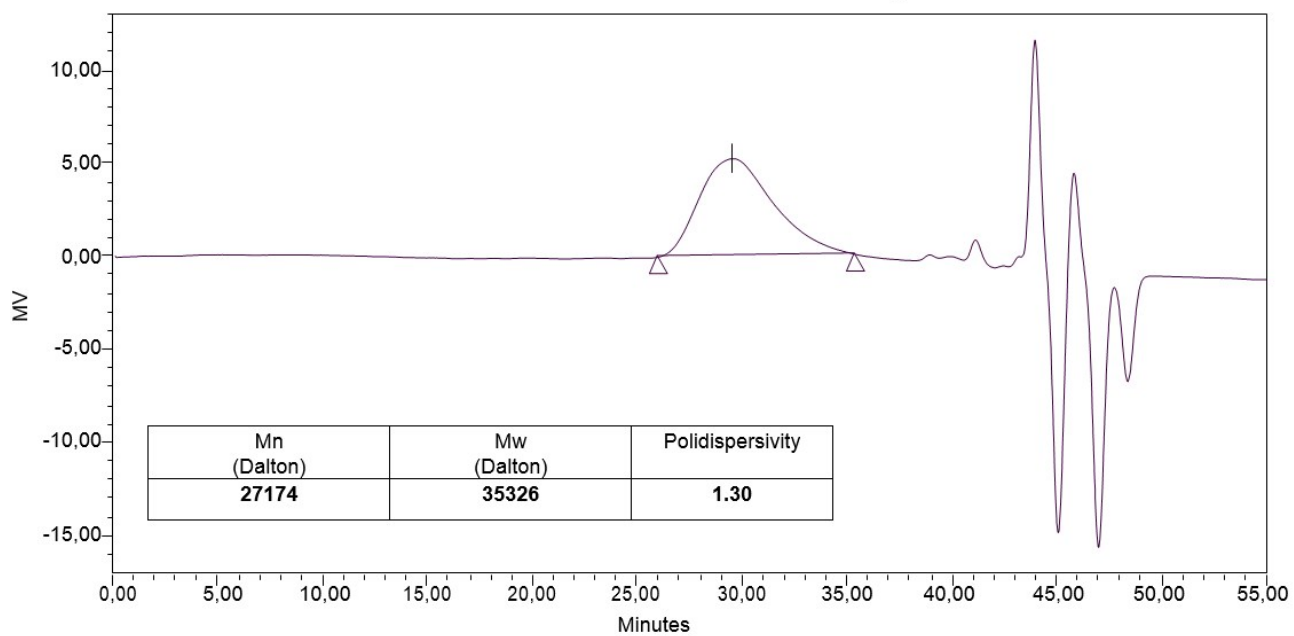


Figure S26. Gel permeation chromatogram of the polymer sample from entry 7 of Table 1.

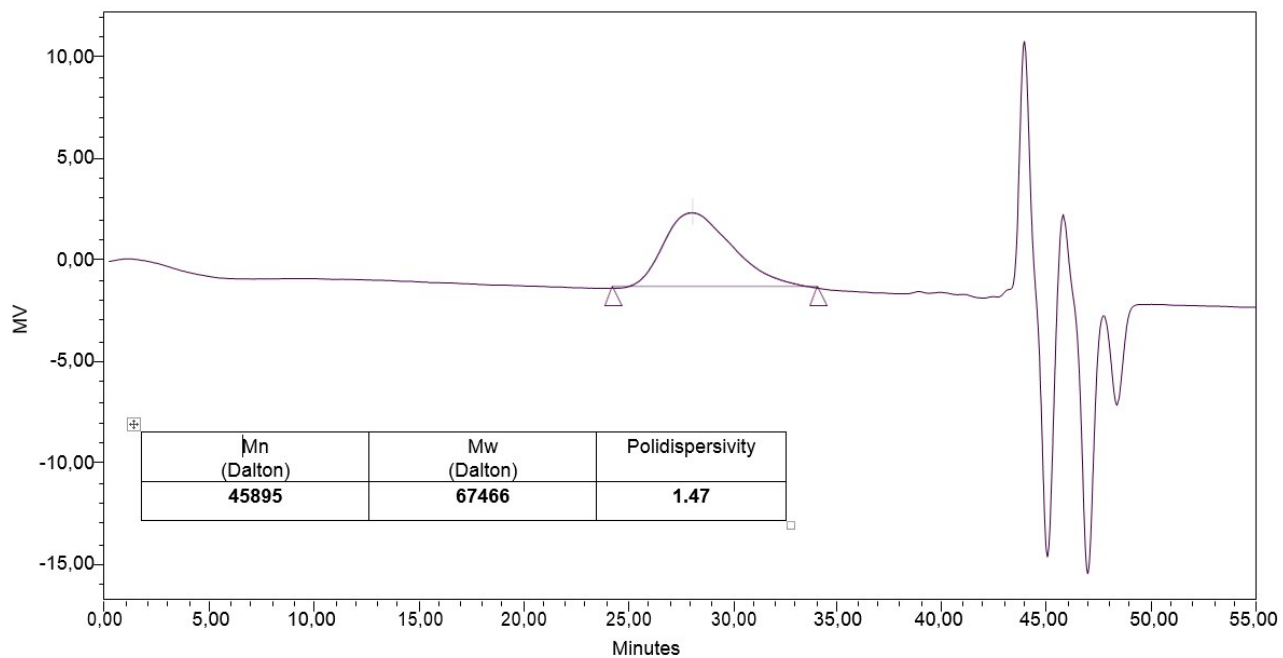


Figure S27. Gel permeation chromatogram of the polymer sample from entry 8 of Table 1.

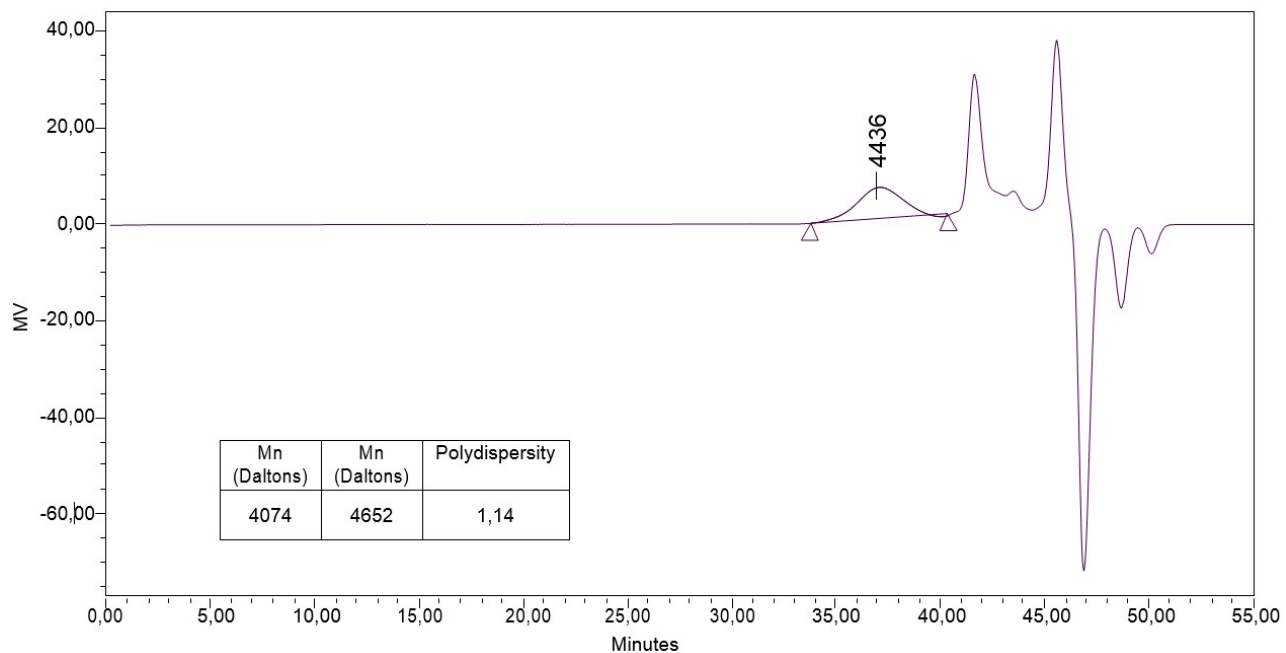


Figure S28. Gel permeation chromatogram of the polymer sample from entry **9** of Table 1.

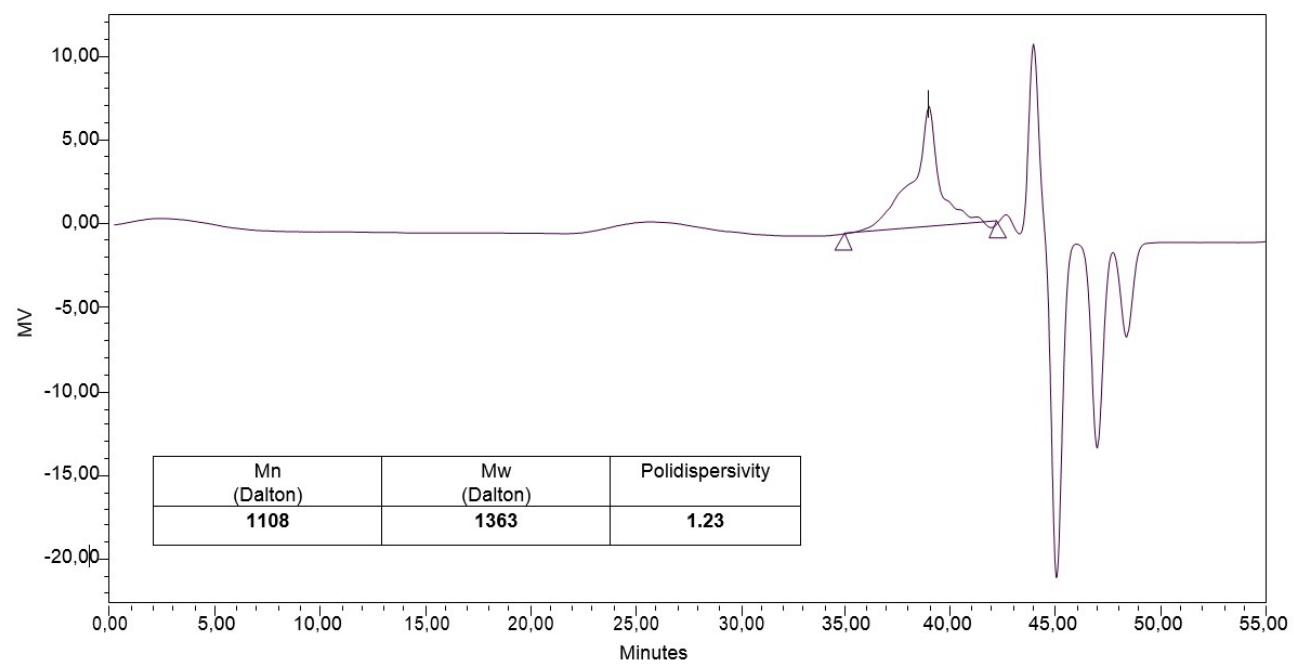


Figure S29. Gel permeation chromatogram of the polymer sample from entry **10** of Table 1.

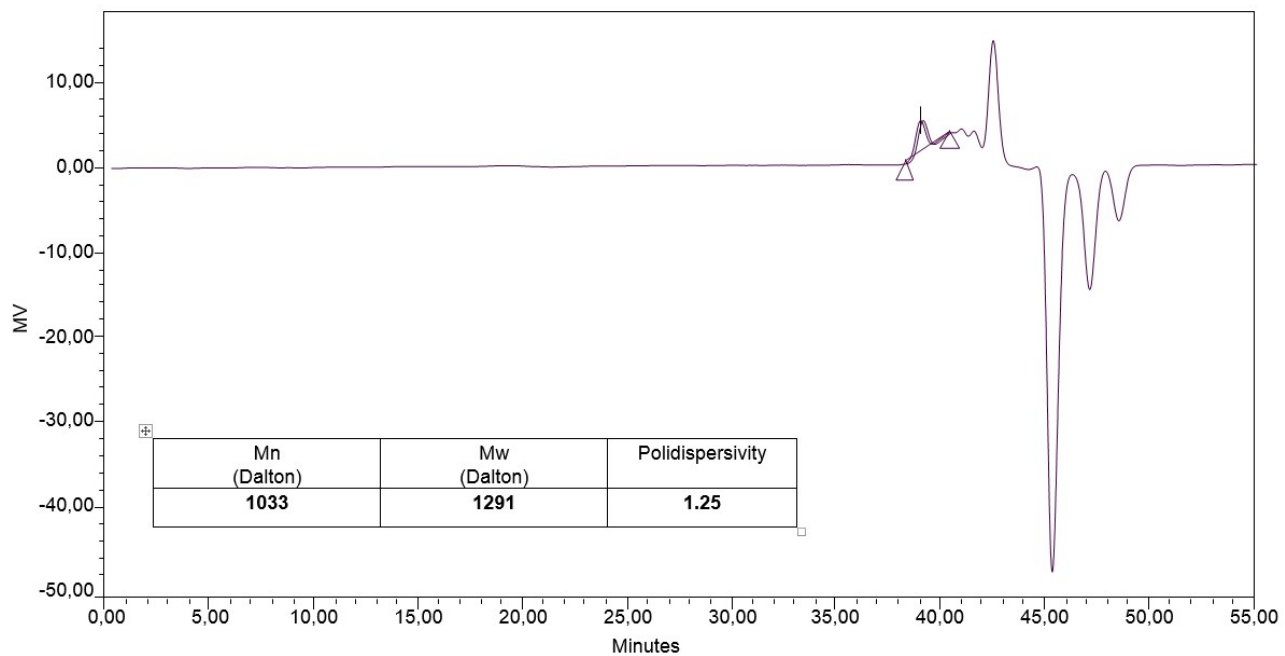


Figure S30. Gel permeation chromatogram of the polymer sample from entry **11** of Table 1.